Available online at www.sciencedirect.com
SCIENCE DIRECT®
Catalysis Today 116 (2006) 206–215
CATALYSIS TODAY
www.elsevier.com/locate/cattod

Catalytic and spectroscopic study of the allylic alcohol synthesis by gas-phase hydrogen transfer reduction of unsaturated ketones on acid–base catalysts

F. Braun, J.I. Di Cosimo *

Catalysis Science and Engineering Research Group (GICIC), Instituto de Investigaciones en Catálisis y Petroquímica-INCAPE- (UNL-CONICET), Santiago del Estero 2654, (3000) Santa Fe, Argentina

Available online 24 May 2006

Abstract

The hydrogen transfer reduction of an α,β-unsaturated ketone, mesityl oxide, was studied on several single oxides in the gas-phase using 2-propanol as a hydrogen source. Selectivity is essentially determined by oxide electronegativity because the reaction proceeds via surface intermediates formed by coordination of 2-propanol and also of C=O and C=C groups of the reactant ketone on the Lewis acid sites provided by the metal cations. Oxides that combine weak Lewis acid cations and strongly basic oxygens such as MgO or Y_2O_3 yield allylic alcohols as the main reduction products of the gas-phase reaction. Adsorption experiments on MgO monitored by FTIR spectroscopy show that competitive 2-propanol and mesityl oxide adsorption on Mg^{2+} cations favors the hydrogen transfer process by a concerted Meerwein–Ponndorf–Verley mechanism whereas strong mesityl oxide adsorption causes simultaneous reduction of C=O and C=C bonds with formation of the saturated alcohol. High reaction temperatures strongly affect the stability of the complex reaction intermediates postulated for saturated and allylic alcohol formation, thereby favoring the simpler double bond migration reaction over the reduction reactions. More electronegative oxides such as ZrO_2 or Al_2O_3 tend to promote the C=C bond reduction giving the saturated ketone. On these oxides, 2-propanol decomposes into acetone and molecular hydrogen at high rates, which is detrimental to carbonyl reduction.

Keywords: Hydrogen transfer; Reduction; α,β-Unsaturated ketone; Electronegativity

1. Introduction

Primary and secondary unsaturated alcohols are important organic intermediates for pharmaceutical, fragrance and food flavoring industries. Among unsaturated alcohols, those derived from allylic ketones (secondary alcohols) are in particular valuable products used in polymer industry. Synthesis of secondary allylic alcohols via allylic ketone reduction by conventional hydrogenation that uses high-pressure H_2 in multiphase batch reactors and noble metal catalysts is hardly achieved because of the higher reactivity of the C=C bond compared with that of the C=O group [1] and because thermodynamics favors hydrogenation of the C=C bond over the C=O bond by ca. 35 kJ/mol [2]. The substituent at the carbonyl hinders coordination of the C=O bond on the surface thereby decreasing the chemoselectivity for the C=O bond saturation [3]. In addition, isomerization of the unsaturated alcohol formed to the corresponding saturated ketone is usually an unavoidable side reaction on metallic catalysts that reduces allylic alcohol yield [4].

Recently, a paper by von Arx et al. [5] reported significant unsaturated alcohol yields for the liquid-phase hydrogenation of ketoisophorone on Pd/Al_2O_3 but for other substrates, the C=C bond was selectively hydrogenated. On the other hand, Milone et al. [6,7] claimed unsaturated alcohol yields as high as 55–65% for liquid-phase hydrogenation of several unsaturated ketones on Au/Fe_2O_3. These two groups accomplished the only successful attempts so far of the use of molecular hydrogen and metallic catalysts for selective hydrogenation of unsaturated ketones toward unsaturated alcohols in *liquid phase*. Still, there is no report in the literature dealing with *gas-phase* hydrogenation of *unsaturated ketones* on metallic catalysts.

Due to the problems arising from gas-phase hydrogenation of unsaturated ketones on noble metals, the hydrogen transfer

* Corresponding author. Tel.: +54 342 4555279; fax: +54 342 4531068.
E-mail address: dicosimo@fiqus.unl.edu.ar (J.I. Di Cosimo).

0920-5861/$ – see front matter © 2006 Elsevier B.V. All rights reserved.
doi:10.1016/j.cattod.2006.01.026

reduction (HTR) has been postulated in the literature as an alternative to conventional hydrogenation process. HTR is a redox reaction in which the reactant is contacted with a hydrogen source (usually a secondary alcohol) without supply of molecular hydrogen. HTR has been explored for the gas-phase C=O bond reduction of α,β-*unsaturated aldehydes* such as citral, cinnamaldehyde, and acrolein [8–10] and may provide a new route for gas-phase reduction of α,β-*unsaturated ketones* in spite of the fact that the substituent to the C=O bond makes the reduction of ketones more difficult [11].

Several applications of the gas-phase HTR of unsaturated cyclic, aryl or allylic ketones can be found in the literature [10,12–14]. However, the catalytic performance toward the allylic alcohol in these examples is less efficient than that for gas-phase reduction of similar unsaturated aldehydes. In addition, catalytic activity and selectivity toward formation of the allylic alcohol largely depends on the chemical nature of the reactant ketone. In spite of these problems, the development of competitive gas-phase continuous flow processes, as an alternative to the liquid-phase batch process would present several technological advantages. However, the gas-phase process faces selectivity problems because of the different reaction pathways possible at high reaction temperatures.

By analogy with homogeneous catalysis, the HTR of unsaturated carbonyl compounds is believed to occur on metal oxides, zeolites or mesoporous materials via a Meerwein–Ponndorf–Verley (MPV) mechanism, which involves the selective reduction of the C=O bond, preserving the other reducible functional groups [14–16]. The chemoselectivity of this process arises from the fact that the mechanism proceeds by hydride transfer from the alcohol via a cyclic six-membered intermediate, in which both reactants are coordinated to a metal cation [17]. However, efforts devoted to elucidate the Lewis acid requirements of the metal cation that promotes this reaction and the role played by those acid properties in the surface coordination of both reactants are still needed.

In a previous paper [18] we studied the gas-phase HTR of an α,β-unsaturated ketone, mesityl oxide (4-methyl-3-penten-2-one) with 2-propanol toward the unsaturated alcohol (4-methyl-3-penten-2-ol), Eq. (1), on Mg-based mixed oxides. We found that on Mg–Al mixed oxides mainly the saturated ketone and the saturated alcohol were obtained. Incorporation of a metal such as copper in the catalyst formulation causes the C=C bond reduction to occur at high rates, thereby shifting the reaction pathway toward the saturated ketone. We interpreted those results in terms of the role played by the different surface species (cationic or metallic) in the coordination of the unsaturated bonds and in the dissociation of 2-propanol, which proved to be detrimental to allylic alcohol synthesis.

We also studied the competitive reactions that might take place on MgO in the gas-phase leading to allylic alcohol and other compounds [19] and by varying the contact time, reaction temperature, alcohol/ketone ratio and type of hydrogen donor we determined the optimum conditions for a maximum allylic alcohol yield of 42%.

In this paper, we continued our study of the gas-phase HTR of mesityl oxide using 2-propanol as a hydrogen source on different single-metal oxides. We have discussed the effect of varying systematically the oxide acid–base properties on the reactivity and selectivity of this reaction. By a combination of catalytic results and adsorption experiments by FTIR spectroscopy we identified reaction intermediates and analyzed stability of these species at different reaction conditions.

Our goal was to elucidate the reaction mechanisms leading to allylic alcohol and to saturated compounds and to ascertain the nature of the surface intermediates and surface active sites that promote these reactions on catalytic materials with different acid–base properties.

2. Experimental

2.1. Catalyst synthesis

High surface area pure MgO was prepared by hydration with distilled water at room temperature of commercial MgO (Carlo Erba, 99%, 0.2% Na, 27 m^2/g) and further decomposition in N_2 at 773 K. Details are given elsewhere [20]. Alumina, ZnO, Y_2O_3 and CeO_2 precursors were prepared by precipitation method at a constant pH of 10. An aqueous solution of the metal cation nitrate was contacted with a basic solution of K_2CO_3 and KOH by dropwise addition of both solutions into a stirred beaker containing 350 cm^3 of distilled deionized water held at 333 K. The precipitates formed were aged in their mother liquor for 2 h at 333 K and then filtered, washed with boiling distilled water until K^+ was no longer detected in the filtrate, and dried at 348 K overnight. The ZrO_2 precursor, i.e., $Zr(OH)_4$ was obtained by precipitation of zirconium oxychloride with ammonium hydroxide. All these precursors were decomposed in N_2 or air at 723–773 K overnight in order to obtain the corresponding oxides.

2.2. Catalyst characterization

BET surface area (S_g) was measured by N_2 physisorption at its boiling point using a Quantachrome Nova-1000 sorptometer.

The total CO_2 adsorption site density and binding energies were obtained from temperature-programmed desorption

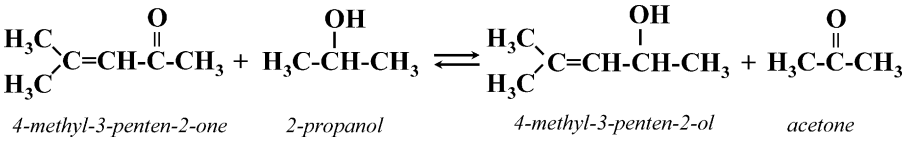

(1)

(TPD) of CO_2 preadsorbed at room temperature. Sample (150 mg) was pretreated in N_2 at 773 K for 1 h and then exposed to a flow of 100 cm^3/min of 3.09% CO_2/N_2 at room temperature until saturation coverage was reached. Weakly adsorbed CO_2 was removed by flowing N_2 and then the temperature was increased to 773 K at 10 K/min. The evolved CO_2 was converted to methane on a methanation catalyst (Ni/Kieselghur) operating at 673 K and monitored using a flame ionization detector.

Acid site densities were determined by using TPD of NH_3. Samples (150 mg) were treated in He (~100 cm^3/min) at 673 K for 0.5 h and exposed to a 1.01% NH_3/He stream at room temperature until surface saturation. Weakly adsorbed NH_3 was removed by flowing He at 60 cm^3/min for 0.5 h. Temperature was then increased to 673 K at 10 K/min, and the NH_3 concentration in the effluent was measured by mass spectrometry (MS).

The structure of CO_2 chemisorbed on the oxides was determined by infrared spectroscopy (IR). Details are given elsewhere [21]. Similarly, the chemical nature of the acid sites present on the oxides was determined by IR of pyridine preadsorbed at room temperature and evacuated at increasing temperatures. Pyridine adsorption spectra were recorded at room temperature. Surface species resulting from adsorption of 2-propanol, mesityl oxide and a mixture of both were identified by IR spectroscopy. All the FTIR experiments were conducted with a Shimadzu FTIR-8101M spectrophotometer using an inverted T-shaped Pyrex cell containing the sample wafer. The two ends of the short arm of the T were fitted with CaF_2 windows. The adsorbates were previously degassed in situ with freeze–pump–thaw cycles. Samples were pressed in 15 mg wafers and degassed in vacuum at 773 K for 1 h and then cooled down to room temperature. The spectrum of the pre-treated catalyst was then taken. After admission of the adsorbate at room temperature, spectra were taken sequentially at increasing adsorption times for 15 min. Samples were then evacuated for 15 min at room temperature and the resulting spectrum was recorded. Spectra of the adsorbed species were obtained by subtracting the catalyst spectrum.

2.3. Catalytic testing

Catalytic tests were conducted at typically 523 K and atmospheric pressure in a fixed bed reactor. Sample sieved at 0.35–0.42 mm was pretreated in N_2 at 773 K for 1 h before reaction in order to remove adsorbed H_2O and CO_2.

The reactants, mesityl oxide, MO (Acros 99%, isomer mixture of mesityl oxide/*iso*-mesityl oxide = 91/9) and 2-propanol, 2P (Merck, ACS, 99.5%) were introduced as a mixture with the proper molar composition via a syringe pump and vaporized into flowing N_2 to give a N_2/2-propanol = 12 M. Reaction products were analyzed by on-line gas chromatography in a Varian Star 3400 CX chromatograph equipped with a flame ionization detector and a 0.2% Carbowax 1500/80–100 Carbopack C column. Main reaction products from MO conversion were identified as the two unsaturated alcohol isomers (UOL_1, 4-methyl-3-penten-2ol and UOL_2, 4-methyl-4-penten-2ol), *iso*-mesityl oxide (*i*-MO), methyl isobutyl ketone (MIBK) and methyl isobutyl carbinol (MIBC). Aldol condensation products are identified as AC. Acetone (DMK) was produced by 2P oxidation in HTR reaction, Eq. (1). Small amounts of propylene were formed by 2P dehydration.

Selectivities (S_i, carbon atoms of product *i*/carbon atoms of MO reacted) were calculated as $S_i = F_i N_i / \sum F_i N_i$ where F_i is the molar flow of a product *i* formed from MO and N_i is the number of carbon atoms in product *i*. Due to catalyst deactivation, the catalytic results reported here were calculated by extrapolation of the reactant and product concentration curves to zero time on stream. Then, X and S represent conversion and selectivity at $t = 0$, respectively.

3. Results and discussion

3.1. Catalyst acid and base properties

The BET surface area, electronegativity and base site density of the different oxides used in this work are reported in Table 1. Oxide electronegativities (χ_{oxide}) were calculated as the geometric mean of the atomic electronegativities using the Pauling's electronegativity scale. For an oxide with the formula M_nO_x, the bulk oxide electronegativity will be [22,23]:

$$\chi_{oxide} = [(\chi_M)^n \quad (\chi_O)^x]^{1/(n+x)}$$

The total amount of desorbed CO_2 was measured by integration of TPD curves. The resulting values are reported in Table 1. The CO_2 desorption rate as a function of sample temperature, Fig. 1, shows that the total base site density (area under the TPD traces) depended on the acid–base properties of the oxide metal cation so that total base site density decreased with increasing oxide electronegativity.

The complex TPD profiles of Fig. 1 reveal the presence of surface base sites that bind CO_2 with different strengths. The TPD traces of Fig. 1 also show that the binding energies of adsorbed CO_2 species are affected by the electronegativity of the metal cations. MgO contains not only weak (CO_2 desorption temperature ≈400 K) and medium-strength (≈450 K) but also high-strength base sites (≈550 K). In previous work [21,24], we identified by FTIR of preadsorbed CO_2, the chemical nature of these base sites and also determined the following base strength order for them: low coordination O^{2-} anions > oxygen in Mg^{2+}-O^{2-} pairs > OH groups. Only low-electronegativity oxides such

Table 1
Catalyst physicochemical properties

Catalyst	S_g (m^2/g)	Electronegativity (Pauling unit)	Base site density[a] (μmol/m^2)
MgO	136	2.12	5.6
Y_2O_3	54	2.27	4.8
CeO_2	75	2.37	1.8
ZnO	12	2.38	<0.1
ZrO_2	49	2.51	0.3
Al_2O_3	300	2.54	0.1

[a] By TPD of CO_2.

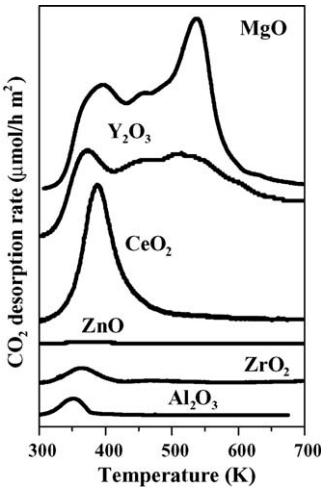

Fig. 1. TPD profiles of CO_2 on oxides with different acid-base properties. CO_2 adsorption at 298 K, 10 K/min heating rate.

as MgO and Y_2O_3 contain strong base sites, as indicated by the high-temperature peak of the TPD traces. More electronegative oxides were weakly or moderately basic. No CO_2 desorption signal could be detected for ZnO.

Fig. 2 compares the IR spectra after pyridine adsorption and evacuation at room temperature on the most and the least electronegative oxides of this study, Al_2O_3 (spectrum a) and MgO (spectrum c), respectively. On both oxides pyridine coordinates on the Lewis acid sites provided by the metal cations as indicated by the bands at 1604–1615 and 1445–1450 cm^{-1} [25–27] corresponding to the ring-breathing (ν_{CCN}) vibrations. On Al_2O_3, a weak H-bonded pyridine band was measured at 1596 cm^{-1} but the bands typical of strong Brönsted acidity (1650 and 1550 cm^{-1}) were not observed, thereby suggesting that the surface OH groups are not strong enough to protonate pyridine and that alumina is only moderately acidic. Evacuation at 373 K almost completely removed pyridine adsorbed on MgO (spectrum d) whereas after thermoevacuation at 423 K species coordinated to Lewis acid sites still remain on the alumina surface (spectrum b). These results and the higher frequency of the band at ≈1600 cm^{-1} measured for Al_2O_3 suggest that this band is associated to stronger Lewis acid sites than those found on MgO, in agreement with electronegativity calculations.

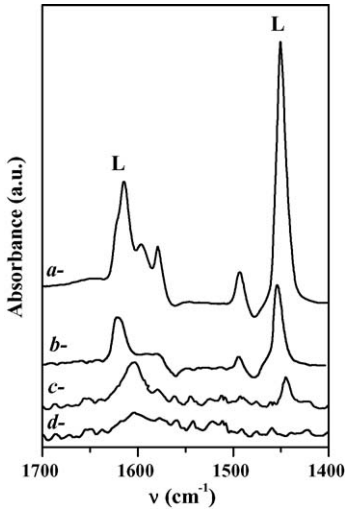

Fig. 2. FTIR spectra of surface species after pyridine adsorption at room temperature and desorption at indicated temperatures. (a) Al_2O_3 298 K; (b) Al_2O_3 423 K; (c) MgO 298 K; (d) MgO 373 K.

Acid site densities determined by integration of the NH_3 TPD profiles (not shown) were measured for MgO and Al_2O_3. The total NH_3 evolved from MgO (0.12 μmol/m^2) includes NH_3 adsorption and decomposition on acid–base pairs that give rise to species such as Mg–NH_2^- whereas an acid site density of 0.81 μmol/m^2 was calculated for Al_2O_3. The NH_3 TPD on Al_2O_3 presents two overlapping signals, a low-temperature peak at about 400 K and a high-temperature peak at 575 K. Since the NH_3 adsorption was performed at room temperature, the low-temperature peak may be attributed to reversible H-bonded adsorption on Brönsted sites whereas the high-temperature peak was assigned to the irreversible coordinated adsorption on Lewis acid sites in agreement with the pyridine adsorption results.

3.2. Reaction pathways

When both reactants mesityl oxide (MO) and 2-propanol (2P) are co-fed to the reactor, in addition to Eq. (1) several parallel or consecutive reactions such as isomerizations and reductions can take place, as depicted in Scheme 1:

(i) MO double bond migration, reaction step (2), leading to isomesityl oxide (*i*-MO), a β,γ-unsaturated ketone. This is

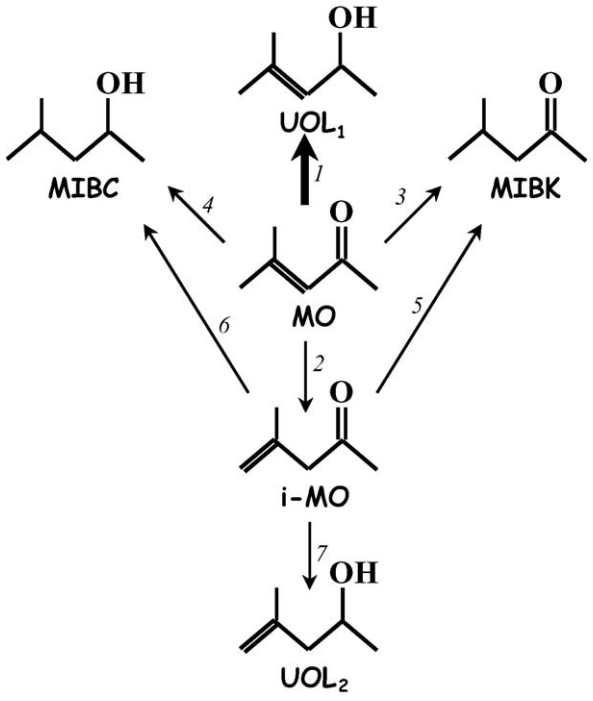

Scheme 1. Reaction network for the gas-phase hydrogen transfer reduction (HTR) of mesityl oxide (MO) with 2-propanol (2P) on acid–base catalysts.

an isomerization step and does not involve the hydrogen donor.

(ii) C=C bond reduction of MO or *i*-MO to MIBK, reaction steps (3) and (5) which present the same stoichiometry as step (1), i.e., one 2-propanol molecule is needed to reduce the C=C bond.

(iii) Simultaneous C=C and C=O bond reduction of MO or *i*-MO to MIBC, reaction steps (4) and (6). Formation of MIBC involves consumption of two hydrogen donor molecules.

(iv) C=O bond reduction of *i*-MO toward UOL_2, reaction step (7). Similarly to step (1), one 2-propanol molecule is consumed in reducing the C=O bond of *i*-MO.

In addition to the reaction steps of Scheme 1, aldol condensation reactions between C_6 carbonyl compounds and DMK (acetone) toward C_9 oxygenates (phorones) are likely to occur at high MO conversion levels on less electronegative oxides, whereas the cleavage of the MO molecule leading to isobutene (*i*-C_4=) was found on more electronegative oxides.

3.3. Effect of oxide electronegativity on catalytic performance

It has been claimed in the literature that a Lewis acid metal is the active center in the homogeneously catalyzed Meerwein–Ponndorf–Verley (MPV) mechanism for selective reduction of the C=O bond [11]. For analogy with homogeneous catalysis, several solid catalytic materials containing Lewis acid metals such as Zr, Hf, B or Sn have been employed in liquid-phase or gas-phase reduction of carbonyl compounds by hydrogen transfer [9,15,16]. However, very little has been said about the acidic nature of that metal as well as about how the acidic properties define surface coordination of the reducible bonds when dealing with unsaturated carbonyl compounds in which competitive C=C or C=O adsorption might take place.

According to the Pauling's definition [28], electronegativity "is the power of an atom in a molecule to attract electrons". Roughly speaking, oxides with a high electronegativity are acidic and those with low electronegativity are basic.

To investigate the effect of the catalyst electronegativity on the activity and selectivity for the HTR of MO with 2P, several catalytic experiments were carried out at similar MO conversion levels (X_{MO} = 25%) on the oxides of Table 1, at 523 K and with a reactant mixture previously vaporized in N_2 (N_2/2P/MO = 93.4/6.6/1.3 kPa). Whereas MgO and Al_2O_3 were very active for this reaction, a contact time (W/F^0_{MO}) 100-fold that of alumina was necessary to reach a MO conversion of 25% on ZnO, probably because of its low surface area (Table 1). Fig. 3A compares the catalytic performance toward reduction products as a function of oxide electronegativity in Pauling units (P.u.). Total selectivity to allylic alcohols (UOL = UOL_1 + UOL_2) and to the saturated alcohol (MIBC) decreased with increasing the oxide electronegativity. Thus, MgO was the best catalyst for reducing the C=O bond of mesityl oxide under gas-phase conditions. Contrarily, selectivity to the saturated ketone (MIBK), increased in going from MgO to Al_2O_3, thereby suggesting that the C=C bond reduction is favored on more acidic oxides. This result is in line with previous work on Mg–Al mixed oxides [18] in which we reported that UOL formation was hampered on Al-containing oxides because Al^{3+} cations tend to promote C=C bond reduction.

The allylic alcohol isomer distribution is also affected by the catalyst electronegativity. Fig. 3B shows that the UOL_1/UOL_2 selectivity ratio decreases on more acidic oxides so that on ZrO_2 and Al_2O_3 the β,γ-unsaturated isomer (UOL_2) was preferentially formed.

In order to get more insight on these results, additional experiments varying the contact time were carried out on Al_2O_3 at 523 K using a reactant mixture with a MO/2P = 1/5 molar ratio. Fig. 4 shows reactant conversions and product selectivities as a function of W/F^0_{MO}. Mesityl oxide conversions (X_{MO}) as high as 85% were achieved on Al_2O_3 at relatively low contact times (Fig. 4A), what reveals the high reactivity of this oxide. However, the selectivity to total UOL did not exceed 13% and reduction of the C=C bond predominated at high conversions yielding MIBK as the main product (Fig. 4B). UOL_1, although formed in low selectivity, is clearly a primary product from C=O bond reduction of MO.

Close inspection of Fig. 4B indicates that *i*-MO formed by double bond isomerization is the main primary product on Al_2O_3 and that most of the reduction products form consecutively from *i*-MO. Double bond isomerization is a fast reaction always present in gas-phase reactions of unsaturated

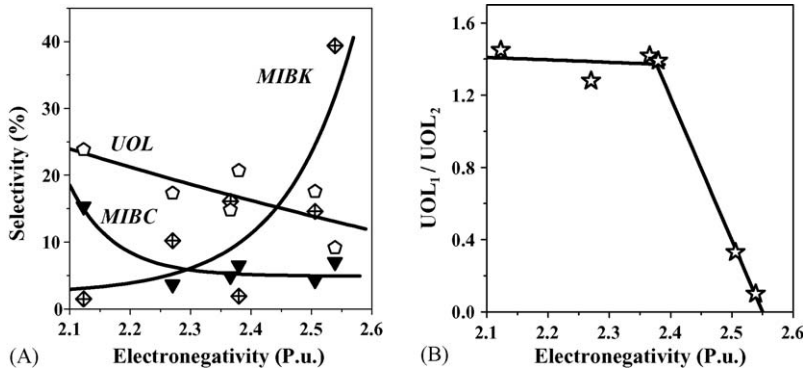

Fig. 3. Effect of the oxide electronegativity on the product distribution of the gas-phase HTR of MO with 2P [T = 523 K, P_T = 101.3 kPa, N_2/2P/MO = 93.4/6.6/1.3 kPa, X_{MO} = 25%]. (A) Selectivity toward reduction products; (B) selectivity ratio of UOL isomers.

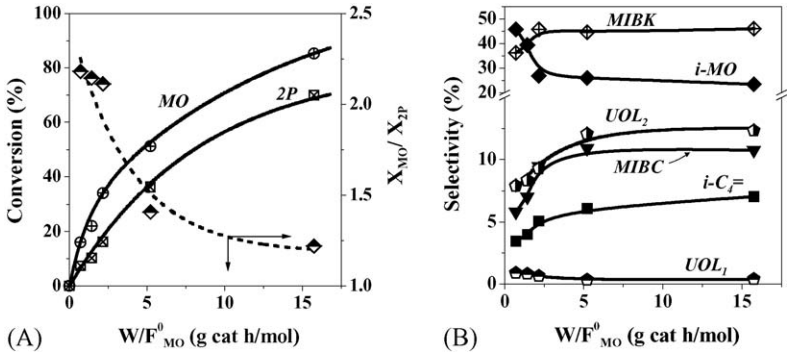

Fig. 4. Effect of contact time on gas-phase HTR of MO with 2P on Al_2O_3 [T = 523 K, P_T = 101.3 kPa, N_2/2P/MO = 93.4/6.6/1.3 kPa]. (A) Reactant conversions; (B) product selectivities.

carbonyl compounds. Similarly to isomerization of olefins on basic oxides, this reaction proceeds via carbanion intermediates [29]. Although the isomerization reaction involves formation of mobile surface protons, it does not necessarily incorporate hydrogen from the hydrogen donor as it may proceed by intramolecular hydrogen transfer. The terminal C=C bond of *i*-MO is kinetically more reactive than that of MO because the lack of methyl substituents facilitates activation on a Lewis acid cation. Thus, on alumina, MIBK probably results from C=C bond reduction of *i*-MO.

Undesirable reduction of the C=C bond on alumina seems to be also related to the high conversion level reached by the hydrogen source. For a reactant mixture with a composition of MO/2P = 1/5 (molar ratio), the expected X_{MO}/X_{2P} conversion ratio should be 5, either for reduction of C=O (Scheme 1, step 1) or C=C (Scheme 1, step 3). However, the measured values of X_{2P} were similar to X_{MO}, and smaller X_{MO}/X_{2P} ratios of around 1.2–2.2 were calculated in the contact time range of this study, thus confirming that 2-propanol conversions on alumina largely exceeded the requirements of hydrogen transfer reductions (Fig. 4A). It was found that on alumina 2-propanol not only participates in HTR reactions, but also in dehydration and dehydration-coupling reactions yielding propene and di-isopropyl ether, respectively. In addition, the concentration of acetone in the reaction products was much higher than the stoichiometrically expected according to the concentration of reduction products, which suggests that 2-propanol was also dehydrogenated to DMK and H_2.

In previous work we have investigated the role of molecular hydrogen on the product distribution of HTR of mesityl oxide [18] and concluded that H_2 decreases UOL and MIBC selectivities at expenses of MIBK formation. In other words, C=C bond reduction takes place at higher rates when molecular H_2 is present in the reaction mixture.

Scheme 2 gives an interpretation, based on the catalytic results, of the surface process leading to C=C bond reduction on electronegative oxides such as alumina. The reaction starts by activation of the MO molecule on an Al^{3+}–O^{2-} pair and proton abstraction at the methyl substituent of the C=C bond. After carbanion formation, fast charge delocalization occurs resulting in double bond migration and formation of *i*-MO. Consecutive adsorption of *i*-MO gives rise to a π_{C-C} complex of the terminal C=C bond on the Al^{3+} cations. On the other hand, 2-propanol is dissociatively activated on an Al^{3+}–O^{2-} pair with formation of a surface 2-propoxide intermediate that in turn converts to acetone. Hydrogen fragments from 2-propanol dissociation can either recombine releasing a H_2 molecule to the gas-phase or migrate to reduce the C=C bond yielding MIBK.

On strongly basic oxides with weak Lewis acidic properties such as MgO and Y_2O_3, experiments varying the contact time showed that the catalytic performance for mesityl oxide reduction was completely different from that of more electronegative oxides, so that the main reduction product was UOL_1 at any conversion level. Conversions and product distribution on MgO as a function of contact time are shown in Fig. 5. Total UOL selectivities of around 50% were obtained with MgO at 523 K, a rather high value for a gas-phase reaction that makes MgO a potentially attractive catalyst for allylic alcohol synthesis from allylic ketones.

Among the reduction products, alcohols (UOL_1, UOL_2 and MIBC) formed in much higher selectivities compared to the saturated ketone (MIBK), thereby suggesting preferential surface activation of the C=O bond of mesityl oxide compared with that of the C=C bond (Fig. 5B). C=C bond reduction was not favored at any conversion level which rules out that MIBK arises from *i*-MO reduction, in spite of the fact that *i*-MO is a primary product. Furthermore, from results of Fig. 5B formation of MIBC by consecutive MIBK or UOL reduction is unlikely. Interconversion between the two UOL isomers is likely to occur because the slight UOL_2 selectivity decrease at

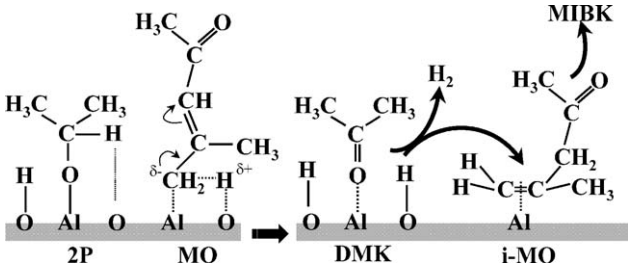

Scheme 2. Surface reaction mechanism leading to MIBK by gas-phase HTR of MO with 2P on Al_2O_3.

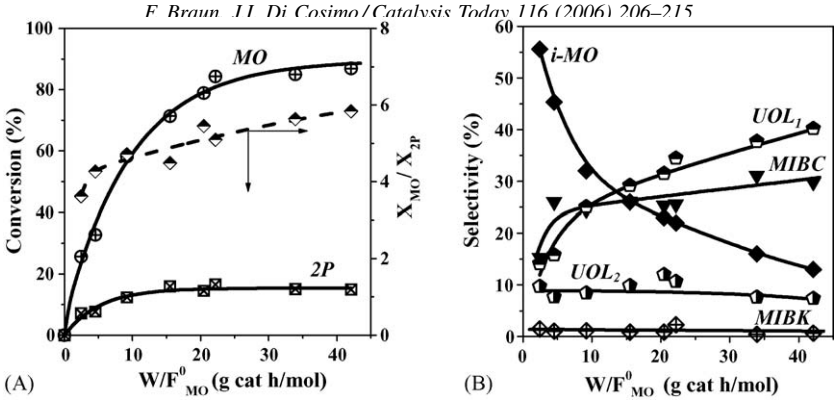

Fig. 5. Effect of contact time on gas-phase HTR of MO with 2P on MgO [T = 523 K, P_T = 101.3 kPa, N_2/2P/MO = 93.4/6.6/1.3 kPa]. (A) Reactant conversions; (B) product selectivities.

high contact times probably reflects conversion into UOL_1, as shown in Fig. 5B.

Reduction of mesityl oxide limited to the C=O bond and therefore leading to alcohols on MgO, seems to be related to the conversion extent of the hydrogen donor, as discussed above for more electronegative oxides, and not to mesityl oxide conversion level. The X_{MO}/X_{2P} ratios as presented in Fig. 5A, were in the range of 4–6, i.e., close to the stoichiometrically expected value of 5. Therefore, 2-propanol converted at lower rates on MgO than on alumina and from the curves of Fig. 5A a 2-propanol initial conversion rate of 992 μmol/hm^2 was measured on MgO, whereas a value of 1600 μmol/hm^2 was determined on alumina from Fig. 4A. Contrarily, mesityl oxide initial conversion rates were similar on both catalysts (832 μmol/hm^2 on Al_2O_3 and 711 μmol/hm^2 on MgO). These results indicate that the lower reactivity of MgO in converting 2-propanol probably renders in a less production of molecular hydrogen and therefore, in a more selective reaction. Then, electronegativity plays a major role in the catalytic performance of single oxides during the gas-phase HTR of mesityl oxide with 2-propanol. Both, 2-propanol conversion extent and preferred activation of one of the unsaturated bonds of mesityl oxide determine selectivity for this reaction.

3.4. Reactant adsorption modes on MgO and product distribution

In order to elucidate the catalytic results obtained on MgO showing preferred formation of alcohols during reaction of mesityl oxide with 2-propanol, additional experiments were carried out varying the reaction temperature. Fig. 6 shows the product distribution in the range of 473–573 K. Although reduction reactions prevailed at all temperatures compared with aldol condensation and isomerization, total selectivity toward reduction products (UOL_1 + UOL_2 + MIBK + MIBC) decreased with increasing temperature. Selective reduction of the C=C bond did not take place at any temperature of this study since MIBK selectivity was negligible.

Simultaneous reduction of C=C and C=O bonds of mesityl oxides (MO and *i*-MO) to MIBC competes with selective reduction of C=O bond of mesityl oxides to the corresponding allylic alcohols but formation of MIBC was clearly not favored at high reaction temperatures (Fig. 6). This result and the fact that MIBC is not formed by reduction of UOL (Fig. 5B) suggest different mesityl oxide surface coordinations and consequently, different reaction intermediates leading to MIBC or UOL formation. Scheme 3 shows the possible surface species resulting from mesityl oxide adsorption on MgO. Whereas the ''on top'', π_{CO} and the di-σ_{CO} structures would be the preferred adsorption modes for the pathway giving unsaturated alcohols, the di-π structure may certainly lead to the saturated alcohol. The fact that Lewis acid cations such as Mg^{2+} stabilize both, the quasi-planar di-π adsorption mode of C=C and C=O bonds and the di-σ_{CO} adsorption mode of C=O bond to about equal extent [30] explains the selectivity problems due to simultaneous formation of MIBC and UOL. However, it seems from results of Fig. 6 that an increase in the reaction temperature is detrimental to the stability of the di-π species and thereby decreases the concentration of surface reaction intermediates leading to MIBC.

Based on our catalytic data we postulate in Scheme 4 the surface process that accounts for C=O bond reduction on MgO. As we discussed previously [18], the reaction proceeds by a Meerwein–Ponndorf–Verley (MPV) mechanism. The homogeneous MPV reaction is catalyzed by metal alkoxides with participation of a Lewis acid center and involves formation of

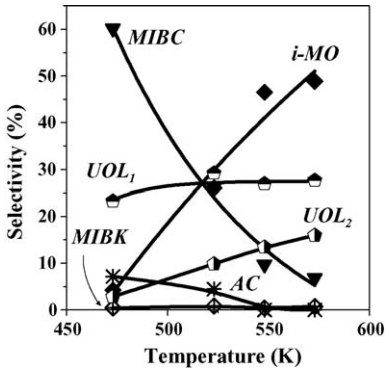

Fig. 6. Effect of reaction temperature on the product distribution of gas-phase HTR of MO with 2P on MgO [P_T = 101.3 kPa, W/F^0_{MO} = 15gh/mol MO, N_2/2P/MO = 93.4/6.6/1.3 kPa].

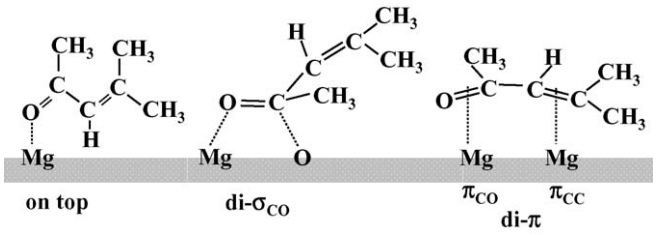

Scheme 3. Adsorption modes of MO on MgO.

a cyclic six-membered intermediate in which both reactants are coordinated to the metal of the alkoxide [17]. A similar intermediate for the heterogeneously catalyzed process can be postulated, as presented in Scheme 4, in which MO coordination takes place *via* an ''on top'' adsorption of the C=O bond on a weak Lewis acid Mg^{2+} cation, whereas 2P adsorbs non-dissociatively on a vicinal Mg^{2+}-O^{2-} pair, giving rise to a cyclic six-atom surface intermediate. Thus, in this concerted mechanism, hydrogen transfers selectively toward the C=O bond, yielding the unsaturated alcohol without participation of surface H fragments from alcohol dissociation.

The complex bimolecular transition state postulated for UOL formation (Scheme 4) is probably not stable enough at high reaction temperatures and the reaction pathway may then shift toward the simpler MO isomerization reaction that does not involve the hydrogen donor. This is supported by results of Fig. 6 in which selectivity to *i*-MO increased with increasing reaction temperature at expenses of reduction products. This has an effect on the distribution of unsaturated alcohol isomers since the selectivity to UOL_2 notoriously increased with temperature, from 3% (473 K) to 16% (573 K), consistently with its direct formation from *i*-MO. As a result, the UOL_1/UOL_2 molar ratio drops from 8.3 (473 K) to 1.7 (573 K), thereby showing that the allylic alcohol distribution may be controlled by temperature.

The species resulting from adsorption of both reactants on MgO were further investigated by FTIR. The spectrum of MgO evacuated at 773 K (not shown) displays an asymmetric peak at about 3739 cm^{-1} (with a shoulder on the lower frequency side) attributed to isolated OH groups on kinks and edges and a broad band centered at 1500 cm^{-1} assigned to residual carbonates [14].

Mesityl oxide was admitted at room temperature in the IR cell containing a 15-mg wafer of MgO previously degassed at 773 K and spectra were then taken during the adsorption at time

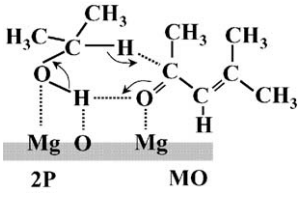

Scheme 4. HTR reaction of mesityl oxide with 2-propanol on MgO. Surface reaction intermediate for allylic alcohol formation by MPV mechanism.

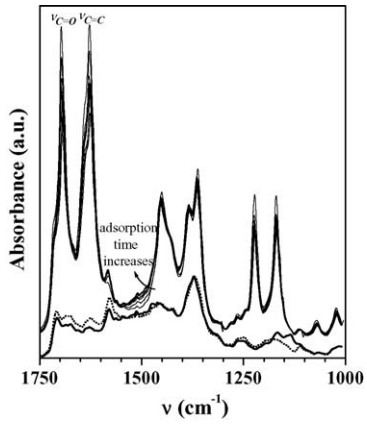

Fig. 7. FTIR spectra of species resulting from admission at room temperature of 1.3 kPa of MO on MgO at increasing adsorption times (thin solid lines); followed by evacuation at room temperature (dotted line); followed by adsorption and evacuation at room temperature of 2P (thick solid line).

intervals of 1.5 min during 15 min (solid thin lines of Fig. 7). Bands remaining on MgO after evacuation at room temperature were in the ν_{OH}, δ_{C-H}, ν_{CHn}, ν_{C-C}, $\nu_{C=O}$ and $\nu_{C=C}$ regions. Spectrum of Fig. 7 (dotted line) shows that after evacuation, bands in the $\nu_{C=O}$ region (1710–1675 cm^{-1}) were shifted to lower frequencies compared to the gas-phase spectra. Several species resulting from surface–carbonyl bond interaction can be identified such as the band at 1710 cm^{-1} assigned to H-bonded C=O [31] and at 1686 and 1675 cm^{-1} corresponding to C=O adsorbed on Lewis centers [32]. The strong band at 1580 cm^{-1} develops with time and is assigned to the enol form of MO coordinated by the C=O bond on a Lewis acid site accompanied by proton abstraction from the MO molecule with concomitant formation of a carbanion stabilized on a Mg^{2+} and a proton on a surface O^{2-} [33,34]. The bands at ≈1420–1450 cm^{-1} correspond to a symmetric and asymmetric deformation (δ_{C-H}) [35]. The intense band at 1370 cm^{-1} is also a symmetric CH_3 deformation [35]. The weak intensity of the $\nu_{C=C}$ band at 1626 cm^{-1} due to C=C bond of MO adsorbed on a Lewis center and the fact that its position is similar to that of C=C bond in gas-phase MO, suggest a weak interaction between the surface Lewis acid Mg^{2+} cations and the C=C bond. Therefore, adsorption of pure mesityl oxide on MgO takes place on Mg^{2+} cations mainly through the C=O bond and to a lesser extent through the C=C bond. It is evident that a di-π adsorption structure such as the one depicted in Scheme 3 is then possible, with the π_{CC} mode being weaker than the π_{CO}.

After evacuation of excess mesityl oxide, the MgO wafer was treated with excess 2-propanol and then the IR cell was once more evacuated at room temperature. The resulting spectrum is displayed as a thick solid line in Fig. 7. The bands of C=O and C=C adsorption on Lewis acid sites (1700–1550 cm^{-1}) were eroded to some extent, what might indicate simultaneous reduction of these bonds in agreement with the catalytic results showing that a surface di-π species leads to unselective reduction of mesityl oxide with formation of MIBC.

In spite of the close resemblance between the dotted line and the thick solid line spectra it is possible to identify in the latter the $\nu_{C-O/C-C}$ stretching vibrations modes of the alkoxide

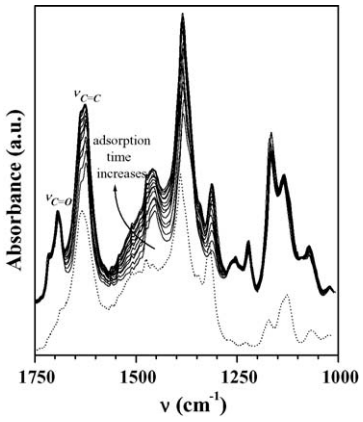

Fig. 8. FTIR spectra of species resulting from admission at room temperature of 3.6 kPa of a MO/2P = 1/5 mixture on MgO at increasing adsorption times (thin solid lines); followed by evacuation at room temperature (dotted line).

resulting from dissociative 2-propanol adsorption on a Mg^{2+}–O^{2-} pair at 1169 and 1135 cm^{-1}. Then, associative adsorption of 2-propanol on a Mg^{2+} cation as depicted in Scheme 4 for selective reduction of the C=O bond is unlikely on a MgO surface pre-covered with strongly bonded mesityl oxide.

In a separate experiment, another MgO wafer was exposed to a mixture of 2-propanol and mesityl oxide (MO/2P = 1/5) in the IR cell and sequential spectra were then taken every minute for 15 min. Results are presented in Fig. 8 (solid lines). Clearly, several bands develop during adsorption mainly in the $\nu_{C=C}$ and δ_{C-H} regions but the latter were largely removed by evacuation at room temperature (dotted line of Fig. 8). The bands in the $\nu_{C=O}$ region assigned to C=O adsorption on Lewis acid cations (1710–1675 cm^{-1}) displayed weak signals after evacuation whereas no band was detected for the enol species (1580 cm^{-1}). The disappearance of the C=O adsorption bands indicates that upon co-adsorption of the reactants, reduction of the C=O bond occurs. This is further supported by the double band observed in the $\nu_{C=C}$ region during adsorption that became a broad band after evacuation probably reflecting formation of the two unsaturated alcohol isomers.

All these results tend to suggest that contrarily to what discussed above for sequential reactant adsorption, when a 2-propanol-rich reactant mixture (like the one used in the catalytic experiments) is adsorbed on MgO, the alcohol and the unsaturated ketone compete for the surface Lewis acid cations forcing the ketone to coordinate by the C=O bond as postulated in Scheme 4 for the concerted mechanism for C=O bond reduction.

4. Conclusions

The carbonyl reduction of unsaturated ketones such as mesityl oxides can be carried out in the gas-phase by a hydrogen transfer process using a secondary alcohol as the hydrogen source. Unsaturated alcohol selectivities of around 50% at 523 K can be obtained on basic catalysts such as MgO, a rather high value for a gas-phase reaction that makes MgO a potentially attractive catalyst for this kind of reactions.

Single oxides exhibit different catalytic performances in the gas-phase hydrogen transfer reduction of mesityl oxide with 2-propanol depending on their acid–base properties. The distinct catalytic behavior of each catalyst is determined by the role played by Lewis acid cations in the coordination of the carbonyl and C=C groups and by stability of reaction intermediates, which are controlled among others, by the catalyst acid–base properties and reaction temperature. Intermediate species of the hydrogen transfer reduction process require that both reactants coordinate on Lewis acid cations.

Oxides of weak Lewis acid cations and strong basic properties such as MgO or Y_2O_3 yield allylic alcohols as the main reduction products. Competitive 2-propanol and mesityl oxide adsorption on Mg^{2+} cations of MgO favors hydrogen transfer by a concerted Meerwein–Ponndorf–Verley mechanism whereas strong mesityl oxide adsorption causes simultaneous reduction of C=O and C=C bonds with formation of the saturated alcohol.

More electronegative oxides such as ZrO_2 or Al_2O_3 tend to promote the C=C bond reduction by a combination of factors that include conversion of the reactant ketone to the β,γ-unsaturated isomer in the first reaction step, followed by consecutive activation of the terminal C=C bond. Also, on more electronegative oxides 2-propanol decomposes at high rates giving acetone and molecular hydrogen. Formation of H_2 is proven to be detrimental to selective carbonyl reduction.

Acknowledgements

Authors thank CONICET, Argentina (Grant PIP 02933/00) and the Universidad Nacional del Litoral (UNL)-Agencia Nacional de Promoción Científica y Tecnológica (ANPCyT), Argentina (Grant PICTO 13234) for the financial support of this work and H. Cabral for technical assistance in obtaining the IR spectra.

References

[1] V. Ponec, Appl. Catal. A 149 (1997) 27.
[2] P. Claus, Appl. Catal. A: Gen. 291 (2005) 222.
[3] R.L. Augustine, Catal. Today 37 (1997) 419.
[4] M.G. Musolino, P. De Maio, A. Donato, R. Pierpaolo, J. Mol. Catal. A: Chem. 208 (2004) 219.
[5] M. von Arx, T. Mallat, A. Baiker, J. Mol. Catal. A: Chem. 148 (1999) 275.
[6] C. Milone, R. Ingoglia, A. Pistone, G. Neri, F. Frusteri, S. Galvagno, J. Catal. 222 (2004) 348.
[7] C. Milone, R. Ingoglia, L. Schipilliti, C. Crisafulli, G. Neri, S. Galvagno, J. Catal. 236 (2005) 80.
[8] M.A. Aramendía, V. Borau, C. Jimenez, J.M. Marinas, A. Porras, F.J. Urbano, Appl. Catal. A: Gen. 172 (1998) 31.
[9] M.A. Aramendía, V. Borau, C. Jimenez, A. Marinas, J.M. Marinas, A. Porras, F. Urbano, Catal. Lett. 50 (1998) 173.
[10] T.M. Jyothi, T. Raja, B.S. Rao, J. Mol. Catal. A: Chem. 168 (2001) 187.
[11] C.F. de Graauw, J.A. Peters, H. van Bekkum, J. Huskens, Synthesis (1994) 1007.
[12] J. Kaspar, A. Trovarelli, M. Lenarda, M. Graziani, Tetrahedron Lett. 30 (1989) 2705.

[13] J. Kijenski, M. Glinski, J. Czarnecki, R. Derlacka, V. Jarzyna, in: M. Guisnet, et al. (Eds.), Heterogeneous Catalysis and Fine Chemicals III, Elsevier Science, Amsterdam, 1993, p. 631.
[14] G. Szollosi, M. Bartok, J. Mol. Catal. A: Chem. 148 (1999) 265.
[15] M. De Bruyn, M. Limbourg, J. Denayer, G.V. Baron, V. Parvulescu, P.J. Grobet, D.E. De Vos, P.A. Jacobs, Appl. Catal. A: Gen. 254 (2003) 189.
[16] A. Corma, M.E. Domine, S. Valencia, J. Catal. 215 (2003) 294.
[17] E.J. Creyghton, S.D. Ganeshie, R.S. Downing, H. van Bekkum, J. Mol. Catal. A: Chem 115 (1997) 457.
[18] J.I. Di Cosimo, A. Acosta, C.R. Apesteguía, J. Mol. Catal. A: Chem. 222 (2004) 87.
[19] J.I. Di Cosimo, A. Acosta, C.R. Apesteguía, J. Mol. Catal. A: Chem. 234 (2005) 111.
[20] J.I. Di Cosimo, V.K. Díez, C.R. Apesteguía, Appl. Catal. A 137 (1996) 149.
[21] V.K. Díez, C.R. Apesteguía, J.I. Di Cosimo, J. Catal. 215 (2003) 220.
[22] R.T. Sanderson, Chemical Bonds and Bond Energy, second ed., Academic Press, New York, 1976.
[23] J. Portier, P. Poizot, J.-M. Tarascon, G. Campet, M.A. Subramanian, Solid State Sci. 5 (2003) 695.
[24] J.I. Di Cosimo, V.K. Díez, M. Xu, E. Iglesia, C.R. Apesteguía, J. Catal. 178 (1998) 499.
[25] C. Morterra, A. Chiorino, G. Ghiotti, E. Fisicaro, J. Chem. Soc. Faraday Trans. I 78 (1982) 2649.
[26] G. Busca, Catal. Today 41 (1998) 191.
[27] G.A.H. Mekhemer, S.A. Halawy, M.A. Mohamed, M.I. Zaki, J. Phys. Chem. B 108 (2004) 13379.
[28] L. Pauling, J. Am. Chem. Soc. 54 (1932) 3570.
[29] H. Hattori, Appl. Catal. A: Gen. 222 (2001) 247.
[30] F. Delbecq, P. Sautet, J. Catal. 152 (1995) 217.
[31] M.I. Zaki, M.A. Hasan, F.A. Al-Sagheer, L. Pasupulety, Langmuir 16 (2) (2000) 430.
[32] A. Panov an, J.J. Fripiat, Langmuir 14 (1998) 3788.
[33] M.I. Zaki, M.A. Hasan, L. Pasupulety, Langmuir 17 (2001) 768.
[34] G. Szollosi, M. Bartók, Catal. Lett. 59 (1999) 179.
[35] S. Xu, B. Zao, Z. Wang, Y. Fan, J. Mol. Struct. 428 (1998) 123.